Effect of Destabilizing Heat Treatment on Solid-State Phase Transformation in High-Chromium Cast Irons

VASILY EFREMENKO, KAZUMICHI SHIMIZU, and YULIIA CHABAK

This work describes the influence of secondary carbide precipitation at destabilizing heat treatment on kinetics of austenite phase transformation at a subcritical range of temperatures in high-Cr cast irons, alloyed with 4 to 6 wt pct of Mn or by complex Mn-Ni-Mo (Mn-Cu-Mo). The samples were soaked at 1073 K to 1373 K (800 °C to 1100 °C) (destabilization) or at 573 K to 973 K (300 °C to 700 °C) (subcritical treatment); the combination of destabilization and subcritical treatment was also used. The investigation was carried out with application of optical and electron microscopy and bulk hardness measurement. Time-temperature-transformation (TTT) curves of secondary carbide precipitation and pearlite transformation for as-cast austenite and destabilized austenite were built in this work. It was determined that the secondary carbide precipitation significantly inhibited the pearlite transformation rate at 823 K to 973 K (550 °C to 700 °C). The inhibition effect is more evident in cast irons alloyed with complex Mn-Ni-Mo or Mn-Cu-Mo. The possible reasons for transformation decelerating could be austenite chemical composition change (enriching by Ni, Si, and Cu, and depleting by Cr) and stresses induced by secondary carbide precipitation.

DOI: 10.1007/s11661-013-1890-9

I. INTRODUCTION

HIGH-Cr cast irons are well known to be widely used for castings that undergo intensive wear (abrasive, erosion, corrosive-abrasion, *etc.*) under operation.[1–4] Excellent wear resistance of these materials is associated with a great amount of hard carbide phases distributed in the metallic matrix. In the as-cast condition, the microstructure of high-Cr cast irons consists of eutectic carbides M_7C_3 and dendrites of primary austenite or pearlite. To obtain the highest wear performance, as-cast high-Cr irons are subjected to heat treatment, which leads to appropriate microstructure change as a result of solid-state phase transformation.

The influence of heat treatment on the microstructure and properties of high-Cr cast irons was comprehensively described in numerous investigations.[5–9] As follows from the published works, two kinds of heat treatment are usually applied for these materials: (1) destabilization heat treatments (heating at 1073 K to 1373 K (800 °C to 1100 °C) with 1 to 6 hours soaking[5–7,10–12]); and (b) subcritical heat treatment, which implies soaking at temperatures 573 K to 973 K (300 °C to 700 °C), that is, below the A_1 critical point.[9,13,14] Destabilization is aimed at destabilizing primary stable austenite to martensite transformation by means of secondary carbide precipitation.[6,10,12] The subcritical heat treatment is performed with the purpose of decreasing the austenite (primary or retained) amount in microstructure or tempering quenched martensite in cast irons.[8] Soaking at a subcritical range of temperatures leads to austenite transformation by eutectoid reaction at 773 K to 973 K (500 °C to 700 °C)[13] or by bainite reaction at 573 K to 723 K (300 °C to 450 °C).[14] The transformation can be preceded by dispersed secondary carbide precipitation effecting an increase of bulk hardness; thereby, subcritical soaking is widely used to improve the hardness and wear resistance of Ni–hard cast irons.[7]

Destabilizing heating is carried out at high temperatures in the range above the A_1 critical point to stimulate Cr-enriched carbide phase (M_7C_3, $M_{23}C_6$) precipitation.[15] According to Bedolla-Jacuinde *et al.*,[10] Kmetic *et al.*,[14] and Maratray,[16] the highest precipitation rate is attributed to a certain temperature—1223 K to 1273 K (950 °C to 1000 °C)—and precipitation kinetics can be presented in time-temperature-transformation (TTT) diagrams by C-shaped curves. The features of the secondary carbide precipitation process and its influence on high-Cr cast iron properties are quite fully described in many works.[12,15–17] The common conclusion is that the secondary carbide occurrence is followed by primary austenite depletion by carbon and carbide-forming alloying elements (Cr, Mn, Mo), which leads to a rise in the martensite start (M_S) temperature. Thus, the primary austenite that is cooled after destabilization can easily be transformed into martensite, resulting in bulk hardness and wear resistance increase.

Destabilizing (D) and subcritical (S) heat treatment could be combined in reversed sequences (D-S and S-D). As was shown by Karantzalis *et al.*,[13] the first one

VASILY EFREMENKO, Professor, and YULIIA CHABAK, Postgraduate Student, are with Priazovskyi State Technical University, Mariupol 87500, Ukraine. Contact e-mail: vgefremenko@rambler.ru KAZUMICHI SHIMIZU, Professor, is with the Muroran Institute of Technology, Muroran, Hokkaido 050-8585, Japan.

Manuscript submitted December 28, 2012.
Article published online July 31, 2013

provides a lower hardness value; therefore, the D-S mode could be proposed as a softening heat treatment to improve the machinability of high-Cr cast irons.[1,18] It is obvious that destabilization (carbide precipitation) should have a sharp effect on primary austenite transformation kinetics at the subcritical range of temperatures. This assumption is based on two points: (1) depletion of austenite by carbon and chromium (manganese and molybdenum) as a result of precipitation; and (2) formation of a large interphase surface as boundaries "secondary carbides–matrix," which are considered as sites for ferrite nucleation. Both of these features can be expected to accelerate pearlite transformation; thus, the austenite elimination during subcritical treatment should be finished faster just after destabilization.

However, despite these considerations, destabilization unexpectedly has the opposite effect. Maratray[16] studied alloying by molybdenum and showed that destabilization at 1273 K (1000 °C) moved the nose of "austenite $\rightarrow$ ferrite + M_3C" transformation farther to the right; this means that the destabilization heat treatment decreases the rate of pearlite transformation. This fact is extremely important in view of its possible influence on microstructure formation when high-Cr cast irons are subjected to softening heat treatment for machinability improvement. The same results were later obtained by Kmetic *et al.*[14] after examination of 18 wt pct Cr-Mo-Ni cast iron. Although the intensive investigations of austenite transformation kinetics in high-Cr cast irons were carried out by many researchers, for example, by Cias,[19] Rozhkova *et al.*,[20,21] and Laird II and Powell,[22] no more data were found illuminating the influence of destabilization on kinetics of subsequent austenite transformation at isothermal subcritical soaking.

Therefore, the objective of the present study is to further investigate the effect of destabilizing heat treatment on kinetics of solid-state phase transformation in high-Cr cast irons (13.7 to 20.1 pct Cr) focusing on verification of Maratray's results as applicable to cast irons alloyed with the increased amount of austenite stabilizing elements (Mn, Ni, Cu).

II. EXPERIMENTAL DETAILS

The studied high-Cr cast irons were melted in a 160-kg capacity induction furnace. Gray cast iron, steel scrap, and Fe-Mn, Fe-Cr, Fe-Mo, Fe-V, and Fe-Si master alloys were used as charge materials. The melt was poured at 1673 K to 1723 K (1400 °C to 1450 °C) directly into sand molds to obtain square bars of 25 × 25 mm. The test specimens of dimension 10 × 10 × 2 mm were cut from cast bars. The chemical compositions of alloys are presented in Table I.

Three schemes of heat treatment (D, S, and D-S) were used in the present work. Scheme D was a destabilization heat treatment: as-cast specimens were soaked at 973 K to 1373 K (700 °C to 1100 °C) for different times up to 6 hours. Destabilization was carried out in an electric muffle furnace. After heating, the specimens were cooled in water.

Scheme S was a subcritical heat treatment: as-cast specimens were soaked at 573 K to 973 K (300 °C to 700 °C) for times up to 25 hours followed by cooling in water. Short soaking (up to 30 minutes) was carried out in an electric salt bath (molten mixture of $NaNO_2$ and K_2NO_3 with ratio 1:1), and longer soaking was fulfilled in the electric muffle furnace. The stability of temperature in the bath and furnace was automatically controlled with an accuracy of ± 5 deg.

The scheme D-S was a combination of destabilization and subcritical treatment. As-cast specimens were held in a furnace at 1223 K (950 °C) for 2.5 hours and after that immediately transferred into the salt bath (or furnace) followed by S heat treatment.

Heat treatment schemes D, S, and D-S were applied to A, B, and C alloys. D and E alloys were D-S heat treated according to the schedule given subsequently. Two specimens of each alloy were used for each soaking time in order to average the results obtained.

The microstructure was examined using an optical microscope (NIKON* Eclipse L150) and a scanning electron microscope (SEM, JEOL** JSM-6510) equipped with an energy dispersive spectroscopy (EDS) system. The microstructure observation was performed on specimens etched by 4 pct nital solution. Phase transformation volume estimation was based on pearlite volume fraction measurement. The latter was carried out according to the point counting method on micrographs using a transparent grid. Each volume fraction value is the average of 20 micrographic observations (the micrograph shows the surface area of size 260 μm in length and 200 μm in width). The confidence

*NIKON is a trademark of Nikon Corporation, Tokyo.

**JEOL is a trademark of Japan Electron Optics Ltd., Tokyo.

Table I. Chemical Compositions of the Alloys Studied (Weight Percent)

Alloy	C	Cr	Si	Mn	Ni	Mo	Cu
A	2.71	14.80	0.60	2.20	0.97	0.40	0.02
B	2.70	13.70	1.30	4.05	0.08	0.01	0.03
C	2.93	16.20	2.20	3.08	0.05	0.90	0.79
D	2.56	17.51	0.90	5.67	0.02	0.02	0.03
E	2.46	20.10	1.19	5.87	0.04	0.01	0.02

interval for the volume fraction measurement varied within the 2.5 to 4.7 vol pct range.

EDS microanalysis was used to determine the chemical composition of the metallic matrix. The positions for measurement were chosen in the central area of dendrites at a distance from secondary carbides. The data of Mn, Cr, Ni, and Si content were obtained by averaging 10 measurement results (both for as-cast and destabilized specimens) with a confidence interval in the range of 0.050 to 0.535 wt pct.

The bulk hardness measurement was fulfilled by the Rockwell method with scale C. Five tests were completed for each specimen. The confidence interval for the hardness measurement was 0.35 to 0.50 HRC.

III. RESULTS AND DISCUSSION

A. *As-Cast Alloy Microstructure*

The microstructure of the as-cast alloy is presented in Figure 1. Alloys A, B, D, and E have a similar microstructure consisting of austenitic dendrites, bordering on "austenite + M_7C_3 carbide" eutectic colonies (Figures 1(a), (b), and (d)); thus, these alloys should be attributed to hypoeutectic white cast irons. The total amount of eutectic carbides in A, B, D, and E alloys varies in the range of 25 to 31 vol pct; no influence of the alloys' chemical composition on the carbide volume fraction was observed. Due to the higher content of alloying elements, which are known to inhibit phase transformation (Mn, Ni, Mo), the austenite is fully retained in the metallic matrix of all alloys during cooling in the process of crystallization.

As follows from Figure 1(c), alloy C is hypereutectic white cast iron, which can be distinguished by the presence of large primary carbides M_7C_3 of elongated hexagonal prism shape surrounded by "austenite + M_7C_3" eutectic; austenite areas are also discerned in alloy C between primary carbides and eutectic colonies. These microstructural features are caused by higher carbon content (2.93 wt pct) and silicon content (2.2 wt pct); the latter element is found to reduce carbon concentration in eutectics, which results in the increase of the carbide volume fraction.[22] Due to the presence of Ni (3.08 wt pct), Cu (0.79 wt pct), and Mo (0.90 wt pct), the austenite remains untransformed in as-cast alloy C.

In alloy B (Figure 1(b)), a small amount of pearlite (3 to 5 vol pct) was observed close to the eutectic carbides. No signs of martensite or pearlite presence were found in A, C, D, and E alloys' microstructures.

The bulk hardness of as-cast A, C, D, and E alloys was 45-46 HRC. As-cast alloy B had increased hardness (48.5 to 49 HRC) due to the pearlite presence in microstructure.

B. *Secondary Carbide Precipitation Kinetics at Destabilization*

As-cast alloys A, B, and C were subjected to destabilizing heat treatment (scheme D). The metallographic study shows that destabilization leads to significant

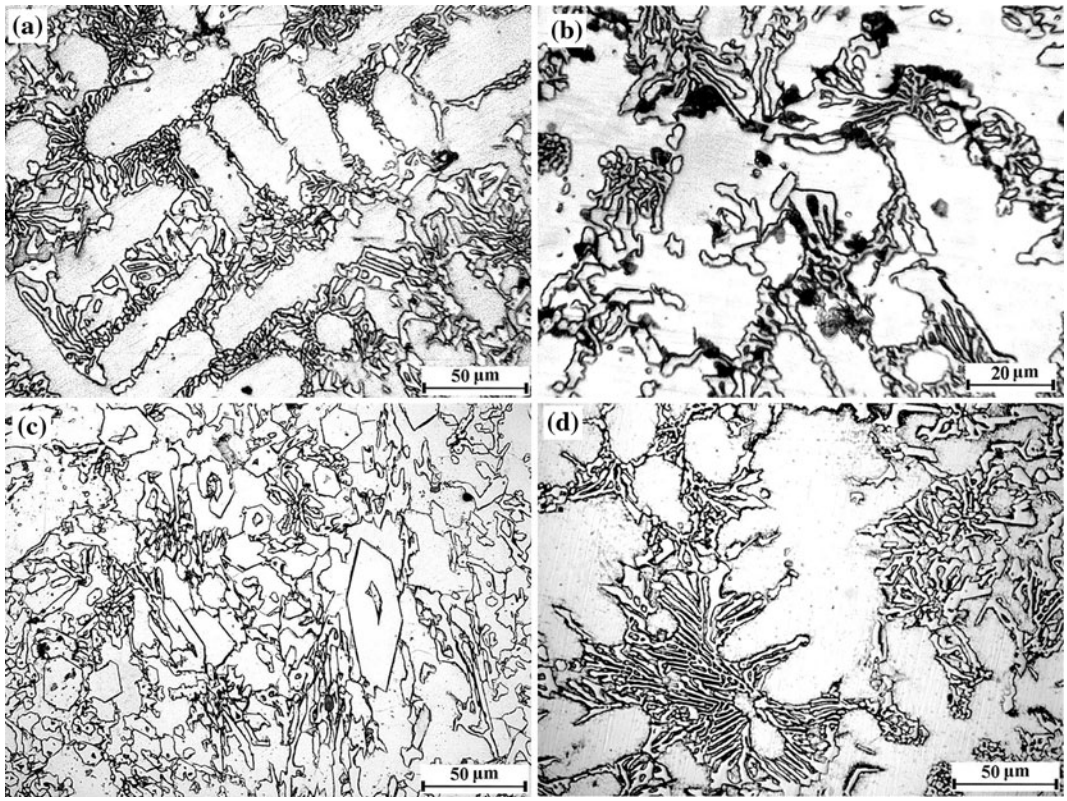

Fig. 1—Microstructure of as-cast alloy (*a*) A, (*b*) B, (*c*) C, and (*d*) D.

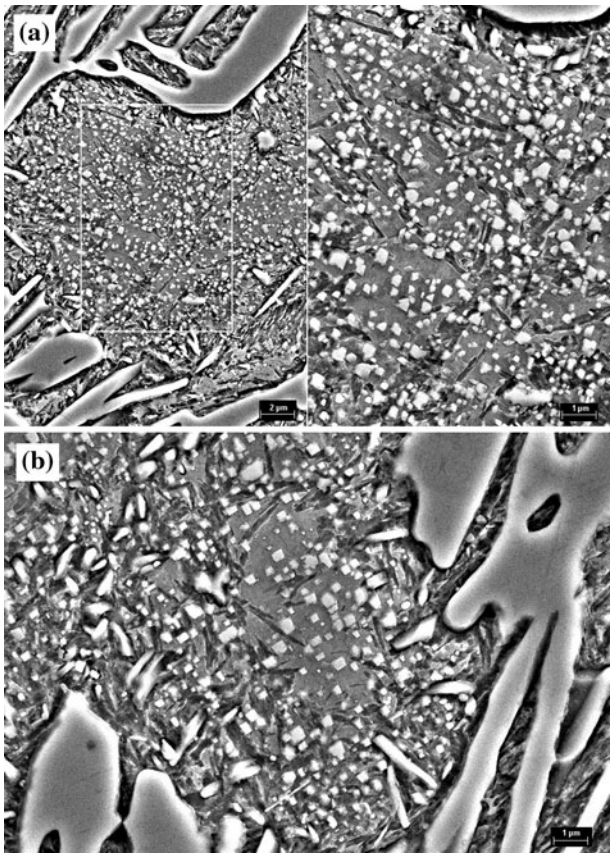

Fig. 2—Microstructure of alloys (*a*) A and (*b*) B destabilized at 1223 K (950 °C) for 2.5 h.

modification of their microstructures in comparison with the as-cast condition. As can be seen from Figure 2, a great amount of granular and needlelike secondary carbides appeared within the austenite dendrites, which resulted in martensite transformation of depleted areas[15] accompanied with a bulk hardness increase.

Figure 3 shows that destabilization treatment significantly influences the hardness of as-cast alloys, with the degree of hardness change depending on temperature and soaking duration. The general trends are as follows. (a) The longer the soaking, the higher the hardness, reaching a maximum of 64, 60, and 59 HRC in alloys A, B, and C, respectively; after long exposure, a slight hardness decrease due to the coarsening effect (or "austenite → pearlite" transformation) in alloy C at 1073 K to 1123 K (800 °C to 850 °C) is observed. (b) When the destabilization temperature grows from 1073 K to 1323 K (800 °C to 1050 °C), the highest hardness value increases first and then decreases; heating at 1223 K (950 °C) provides the highest bulk hardness for all alloys studied.

Alloy B has higher bulk hardness (48.5 to 49 HRC) at the initial stage of destabilization at 1073 K to 1123 K (800 °C to 850 °C) because of the pearlite remaining in the microstructure. When heated at 1173 K to 1273 K (900 °C to 1000 °C), alloy B proceeds quickly through reverse transformation and its initial hardness becomes 46 HRC, which meets the fully austenitic matrix.

In the last stage of soaking, the hardness growth is followed by a certain fall, which is associated with the coarsening of secondary carbides. In alloy C, the drop of hardness during soaking at 1073 K and 1123 K (800 °C and 850 °C) is more significant than in other alloys, which is explained by the fact that the 1073 K to 1123 K (800 °C to 850 °C) interval is close to the critical point A_1 in alloy C, so within this temperature range, the carbide precipitation goes along with the "austenite → pearlite" transformation when the soaking time is more than 40 minutes (at 1073 K (800 °C)) and 80 minutes (at 1123 K (850 °C)). The appearance of pearlite leads to reduction of the martensite volume fraction followed by hardness decreasing in the destabilized alloy C.

As long as the secondary carbide precipitation obviously affects the alloy hardness, the data shown in Figure 3 could be considered as secondary carbide precipitation kinetics. Assuming that the hardness increment is proportional to the precipitation volume and the highest hardness corresponds to the precipitation process completion, we have reconstructed the graphs for hardness into the kinetic curves (Figure 3(d)). This approach to the study of isothermal precipitation kinetics is close to the method[23] based on M_s temperature measurements.

Based on precipitation kinetics, the TTT diagrams for secondary carbide precipitation were built (Figure 4). In Figure 4(c), there are no data concerning 100 pct precipitation volume for 1073 K to 1123 K (800 °C to 850 °C) in alloy C, because "austenite → pearlite" transformation makes this measurement problematic.

As can be seen from Figure 4, the TTT diagrams for all alloys are represented by C-shaped curves, which means that there is a temperature [about 1223 K (950 °C)] that corresponds to the highest rate of secondary carbide precipitation. At other destabilizing temperatures, the precipitation process takes longer. We suggest that the maximum precipitation rate at 1223 K (950 °C) is caused by superposition of two factors that compete with each other when the destabilizing temperature rises. These factors are growth of the diffusion activity of carbide-forming elements (Cr, Mn, Mo) and the increase of carbon solubility in the austenitic phase.

At 1223 K (950 °C), the precipitation process starts after about 10 seconds of soaking for each cast iron; thus, the chemical composition does not affect the incubation period. However, the great difference in finishing time was found: the precipitating finished after 7100, 3300, and 6000 seconds of soaking for alloys A, B, and C, respectively, which means that in the later stages of destabilization, the complex alloying by Mn + Mo + Ni (Cu) makes secondary carbide precipitation more difficult compared to monoalloying by Mn. This occurrence can be attributed to the more effective inhibition of chromium atom diffusion due to the more significant distortion of the fcc lattice, which is particularly evident in the last stage of destabilization, when the formation of new carbide requires a considerable redistribution of chromium atoms within the lattice.

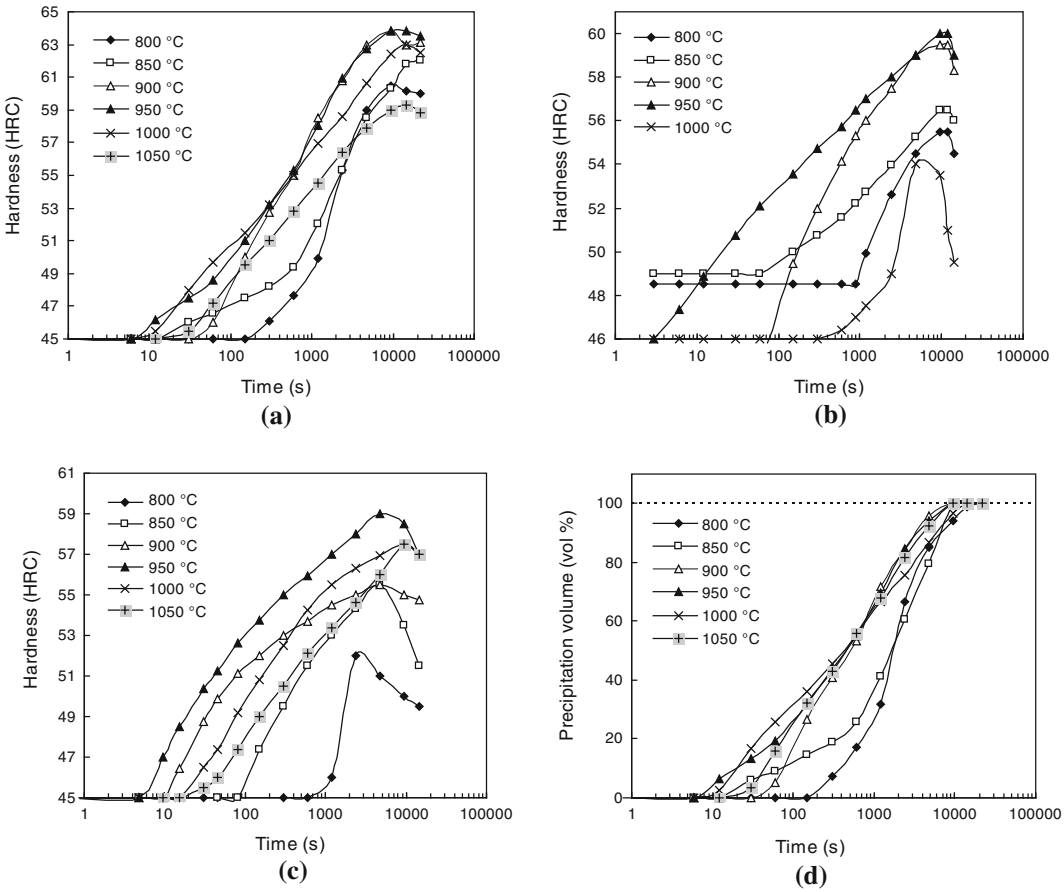

Fig. 3—Effect of destabilization soaking time on bulk hardness of alloys (*a*) A, (*b*) B, and (*c*) C. (*d*) Kinetic curves for secondary carbide precipitation in alloy A.

C. *As-Cast Austenite Transformation Kinetics at Subcritical Temperatures*

The specimens of as-cast alloys were subjected to subcritical heat treatment (scheme S). The microstructure examination revealed that in the temperature range of 573 K to 973 K (300 °C to 700 °C), only pearlite transformation takes place (Figure 5); the pearlite is distinguished as dark areas. SEM observation revealed that pearlite colonies consist of fine plate carbides or curved fiber carbides (of diameter 0.1 to 0.2 μm) distributed in the ferrite matrix (Figure 6). The small nuclei of pearlite colonies were found to appear next to or inside eutectic carbides, *i.e.*, in areas where austenite is depleted in C and Cr[15] (Figure 5(a)). Because they are nucleated, these colonies grow toward the center of dendrites, covering certain austenite dendrites (Figure 5(b)); when soaking time is increased, new colonies appear inside dendrites far from eutectics (Figure 5(c)). However, some austenite areas remain untransformed for long periods of time, indicating high stability presumably due to segregation of Mn, Ni, and Si (Figure 5(d)). After long soaking, almost all austenite was found to have been transformed into pearlite (Figure 5(e)).

No trace of secondary carbide precipitates was observed in alloys A, B, and C at 573 K to 973 K (300 °C to 700 °C). It should also be noted that when soaked up to 25 hours at 573 K to 723 K (300 °C to 450 °C), the bainite transformation in the alloys studied was not found either.

The kinetic curves of pearlite transformation were built by evaluation of micrographs for different soaking times (Figure 7). As can be seen from Figure 7, in alloys A and B, austenite completely transforms into pearlite at 873 K to 973 K (600 °C to 700 °C). At 823 K (550 °C), transformation reaches 60 and 100 vol pct in alloys A and B, respectively. At 773 K (500 °C), the transformation in alloy B proceeds very slowly; in alloy A, the transformation was not observed at 773 K (500 °C).

In alloy C, pearlite transformation is not complete: 10 vol pct of untransformed austenite remains at 873 K (600 °C) and 5 to 9 vol pct, at 923 K to 973 K (650 °C to 700 °C). At 823 K (550 °C), after 25 hours of soaking, the transformation volume is only 25 pct. At lower temperatures 773 K to 573 K (500 °C to 300 °C), the transformation does not take place in this alloy.

The lower part of TTT diagrams (Figure 7) for as-cast alloys was built using kinetic curves. As can be seen from Figure 4, the pearlite transformation differs from secondary carbide precipitation by longer incubation period and lower rate. The highest pearlite transformation rate is attributed to 923 K (650 °C) for all alloys

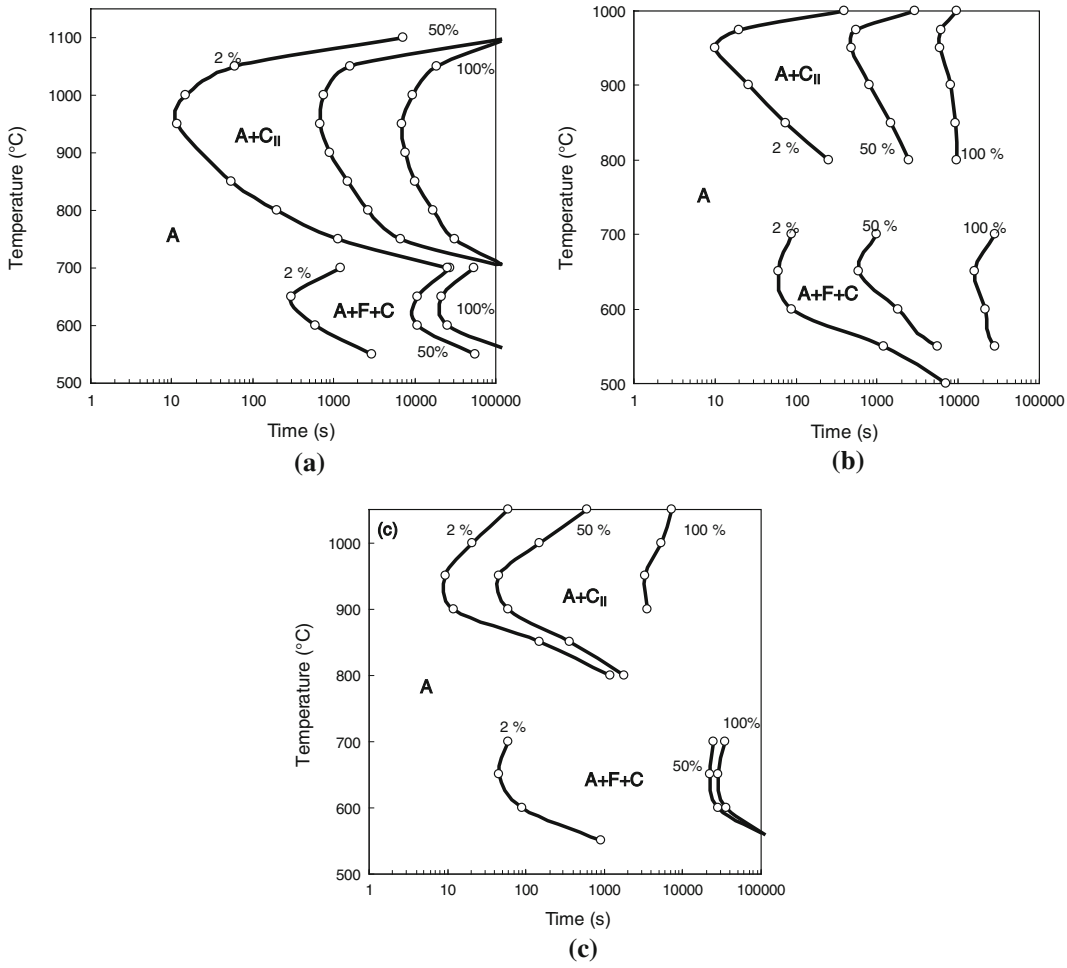

Fig. 4—TTT diagrams for as-cast alloys (*a*) A, (*b*) B, and (*c*) C.

studied. The growth of the austenite decomposition rate along with a decrease of temperature to 923 K (650 °C) is caused by an increasing driving force for γ-Fe $\rightarrow$ α-Fe phase transformation. The induction period corresponding to this temperature is 300, 60, and 45 seconds, for alloys A, B, and C, respectively. The transformation completion time (at 923 K (650 °C)) is 21,000, 10,800, and 27,000 seconds for alloys A, B, and C, respectively. At temperatures below 650 °C, the transformation rate becomes lower due to a decrease of diffusion mobility of carbon atoms and alloying elements.

As-cast austenite in alloy A is the most stable to pearlite transformation. The total amount of austenite-forming elements (Mn, Ni) in alloy A is lower than in alloy B, 3.17 and 4.05 wt pct, respectively. However the incubation period of pearlite transformation in alloy A is 5 times higher compared to alloy B. This finding can be treated as a result of combined alloying by Mn and Ni, which is in good agreement with the conclusions reported in Reference 24. Manganese and nickel delay pearlite transformation due to the reduction of thermodynamic driving force of phase transformation. They mutually reinforce each other, inhibiting ferrite nucleus formation on the interphase boundaries.[25] One should mention that molybdenum (0.40 wt pct) can also contribute to transformation retention in alloy A,[1,26] although the effect is not very significant taking into account its predominant segregation in eutectic carbides.[27]

Alloy C also contains about 4 pct austenite-forming elements (Mn, Cu) as well as a higher amount of molybdenum (0.90 wt pct). However, alloy C is found to have the shortest induction period (60 seconds), which can be explained by higher carbon and silicon content. Both elements are known to increase the eutectic carbide volume fraction, which leads to chromium depletion of the metallic matrix. The decrease of chromium content in the matrix decreases the austenite's stability.[28] Besides, the growth of the carbide volume fraction leads to increased interphase surface, where pearlite can nucleate, which stimulates transformation. At the same time, from Figures 4 and 7, we also can see that alloy C is distinguished from alloy A by a significant transformation slowdown in its later stages. It is manifested in the longest transformation completion time and in untransformed austenite retaining in the alloy C structure. This can be attributed to alloying by copper (0.79 wt pct), which is prone to form clusters enriched by Cu atoms. Austenite demonstrates high stability with respect to pearlite transformation in these segregation zones.

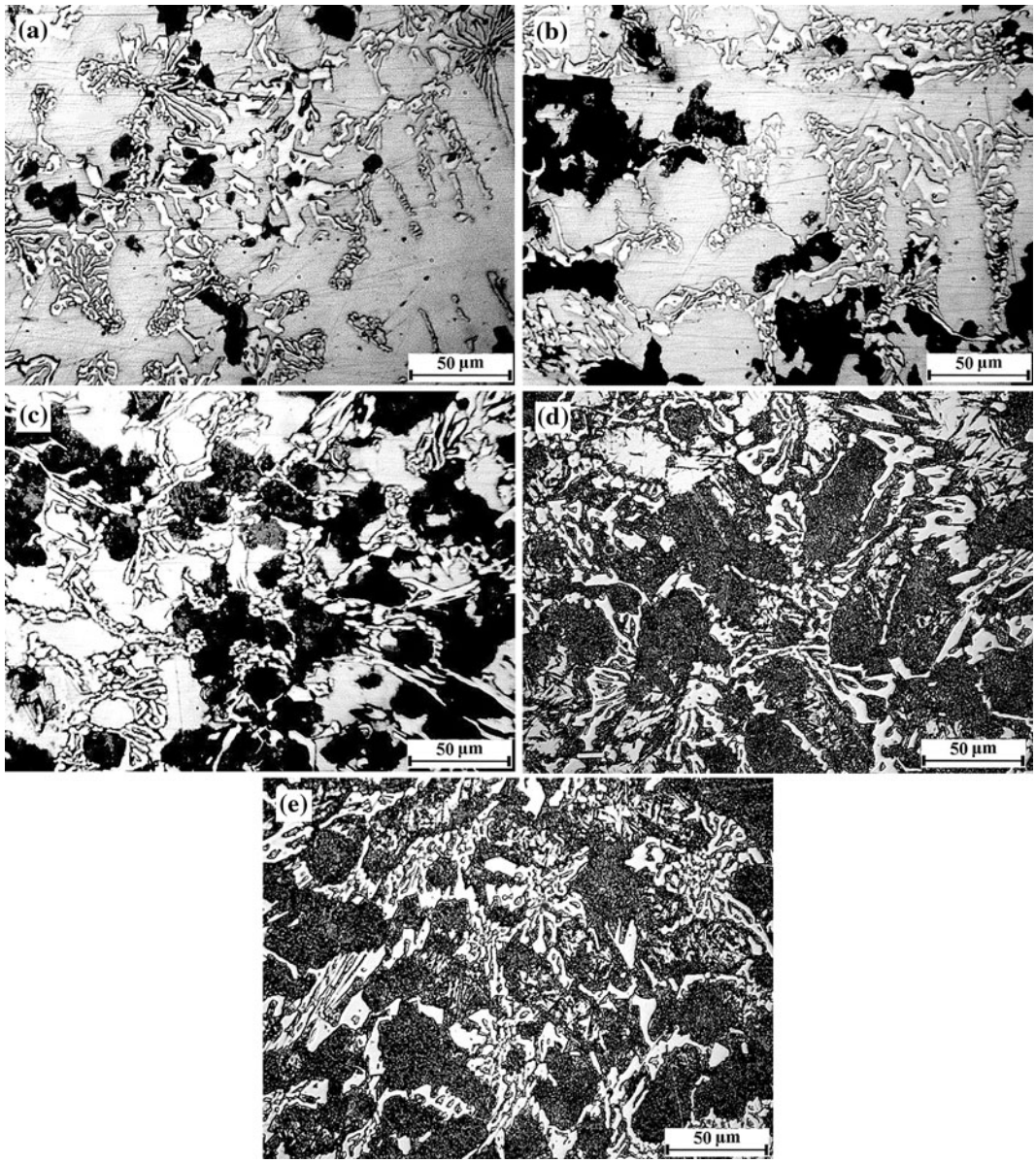

Fig. 5—Progress of "austenite → pearlite" transformation in as-cast alloy A with soaking at 923 K (650 °C) for (*a*) 20 min, (*b*) 1 h, (*c*) 2 h, (*d*) 5 h, and (*e*) 6 h.

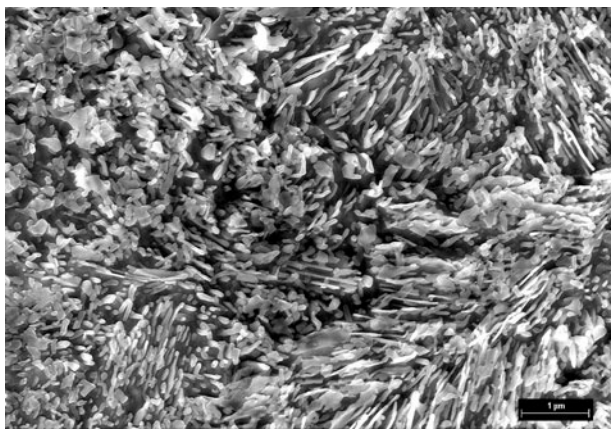

Fig. 6—SEM micrograph of pearlite colonies in alloy A [soaking at 923 K (650 °C, 3 h)].

D. *Destabilized Austenite Transformation Kinetics at Subcritical Temperatures*

In order to clarify the effect of destabilization heat treatment on the kinetics of pearlite transformation, the specimens of alloys were preliminary destabilized by isothermal soaking at 1223 K (950 °C) for 2.5 hours and then subjected to subcritical heat treatment (D-S scheme). The microstructure of the D-S heat-treated specimens is shown in Figure 8. Microstructural observation showed that only pearlite transformation takes place in destabilized alloys during subcritical soaking. Pearlite starts to show up mostly inside the eutectic colonies and right next to the eutectic carbides (Figures 8(a) and (b)). Only after a long soaking time does pearlite appear in the inner zones of the austenitic dendrites (Figure 8(c)).

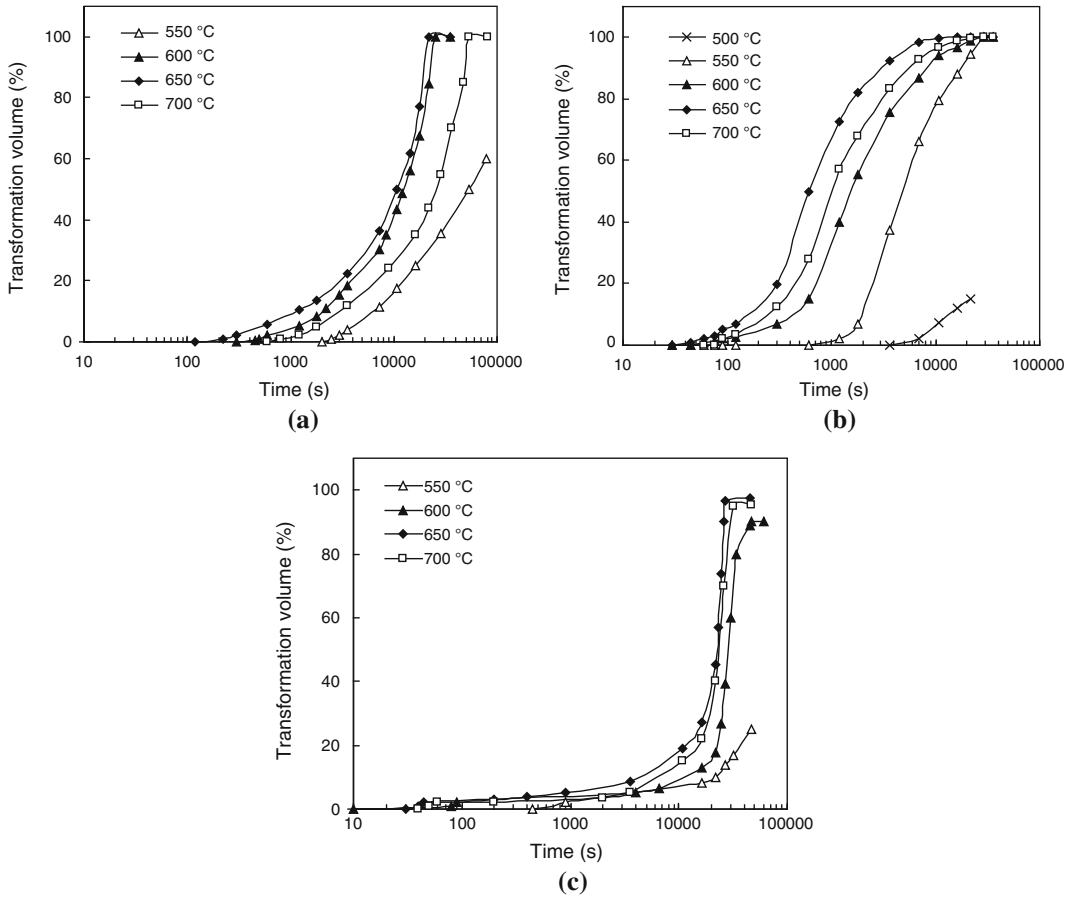

Fig. 7—Kinetic curves for "austenite → pearlite" transformation in as-cast alloys (*a*) A, (*b*) B, and (*c*) C.

The austenite untransformed at subcritical soaking was found to be transformed into martensite when specimens were cooled to ambient temperature. This follows from high bulk hardness of specimens heat treated according to the D-S scheme. As can be seen in Figure 9, the hardness of alloy A is 58 HRC after short subcritical soaking. With the increase of soaking time, the hardness slightly decreases in accordance with pearlite transformation expansion.

TTT diagrams for destabilized austenite transformation were built according to the procedure mentioned previously (Figure 10). The maximum of the transformation rate in destabilized cast iron A is noted for 873 K (600 °C), which is lower than in the as-cast condition. In destabilized cast irons B and C, the "nose" of TTT diagrams corresponds to 923 K (650 °C) and 873 K to 923 K (600 °C to 650 °C), accordingly.

The comparison of the data presented in Figures 4 and 10 allows us to conclude that destabilization considerably slows the solid-state phase transformation, which is fully consistent with the results obtained by Maratray[16] and Kmetic *et al.*[14] The incubation period of transformation increases for all alloys at any soaking temperature. Figure 11 shows the ratio $I_{a\text{-}c}/I_d$, where $I_{a\text{-}c}$ and I_d are the incubation period for the as-cast condition and destabilized condition, respectively. As can be seen, the ratio $I_{a\text{-}c}/I_d$ is 3.3 to 13.3 for alloys A and B; for alloy C, the ratio $I_{a\text{-}c}/I_d$ is much higher, 24.0 to 222.2.

Within 25 hours of soaking, just the very beginning of transformation (2 to 5 vol. pct) was revealed in destabilized alloy C. In alloy A, the transformation went further, reaching 15 vol pct at 873 K to 923 K (600 °C to 650 °C). Most quickly, transformation proceeded in destabilized alloy B, although the incubation period and transformation completion time rose 3.3 to 7.0 times and 1.29 to 1.58 times, respectively, compared with the as-cast state.

Thus, the destabilization-induced effect of transformation deceleration (DIETD) was observed in alloys A through C. To expand the framework of the research and to verify the results obtained, two more high-Cr cast irons (D and E) were studied. These alloys are characterized by higher chromium and manganese content. They were destabilized at 1223 K (950 °C) for 2.5 hours followed by soaking at 923 K (650 °C) for 3 hours (the same subcritical treatment was used for as-cast irons specimens). A comparison of results for as-cast and preliminary destabilized specimens showed that destabilization decreases the pearlite transformation volume in alloys D and E, as was noted for alloys A through C (Figure 12). Thereby, it was concluded that DIETD occurs not only in cast irons with 13.7 to 16.2 pct Cr, but also in the cast irons with higher chromium content

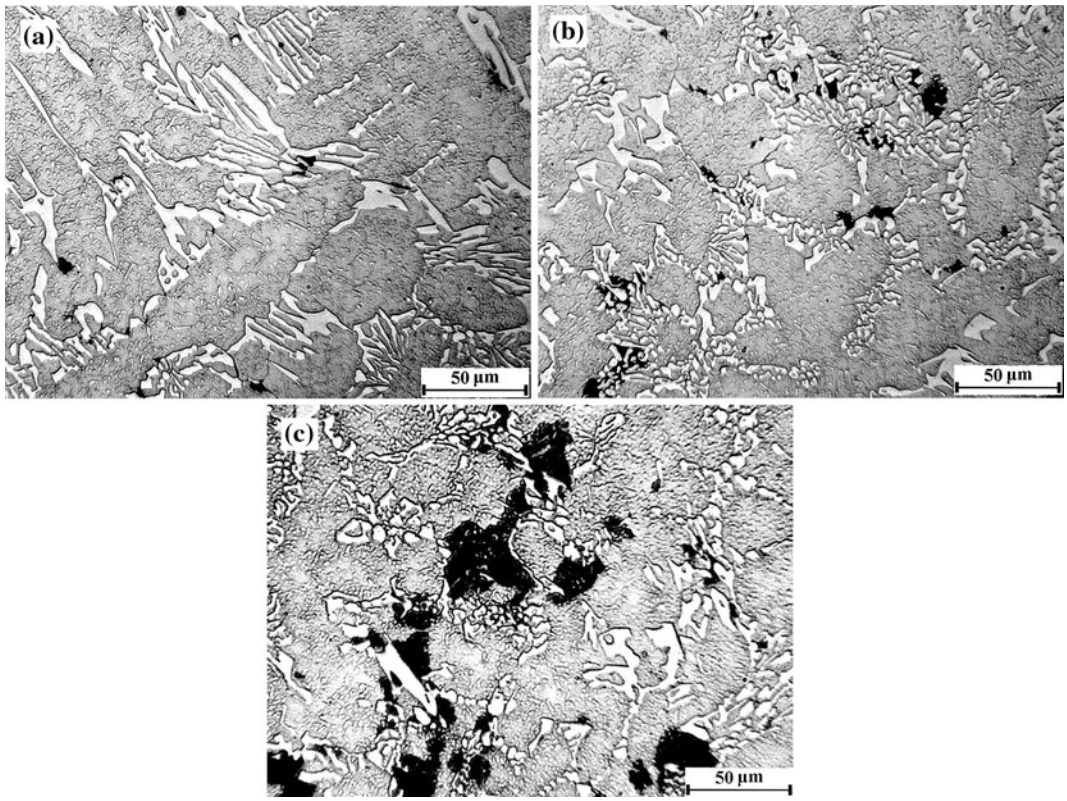

Fig. 8—Progress of ''austenite → pearlite'' transformation in destabilized alloy A after (*a*) 30 min, (*b*) 1 h, and (*c*) 6 h soaking at 923 K (650 °C).

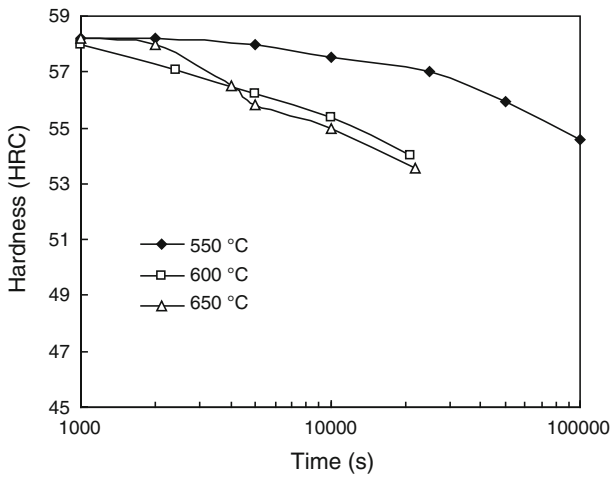

Fig. 9—Effect of subcritical soaking on bulk hardness of preliminary destabilized alloy A.

(17.5 to 20.1 pct) and manganese content (about 6 pct Mn).

The ratio $TV_{a\text{-}c}/TV_d$ for soaking at 923 K (650 °C), 3 hours was calculated for all cast irons studied, where $TV_{a\text{-}c}$ and TV_d represent the transformation volume for the as-cast condition and the destabilized condition, respectively. The ratio $TV_{a\text{-}c}/TV_d$ values are 6.54, 1.35, 9.50, 4.67, and 5.08 for alloys A, B, C, D, and E, respectively. These data show that the transformation deceleration effect grows along with the chromium and manganese content increase (when high-Cr cast irons were additionally alloyed only by Mn). This effect is much stronger for high-Cr cast irons that are alloyed by complex Mn-Ni(Cu)-Mo. It should be noted that cast iron C (Cr-Mn-Mo-Cu) is most sensitive to pearlite transformation inhibition induced by secondary carbide precipitation. After destabilizing, heat treatment alloy C demonstrates the highest stability to pearlite transformation among all alloys studied.

E. *Effect of Destabilization Soaking on Austenite Transformation Rate*

The data described in Section III–D evidently point out that DIETD is affected by secondary carbide precipitation. It was assumed that the degree of transformation deceleration depended on the volume of secondary carbides precipitated. To verify this assumption, an additional heat treatment was used. The specimens of alloys A, B, and C were destabilized at 1223 K (950 °C) for 0.5, 1.0, and 2.5 hours, respectively, and then soaked at 923 K (650 °C) for 3 hours. The microstructure of heat-treated specimens was investigated; the changes in transformation volume depending on the destabilization time are shown in Figure 13. According to these results, one can conclude that increasing destabilization soaking time leads to a reduction of pearlite transformation volume. As Bedolla-Jacuinde *et al.*[10] previously found, there is a direct

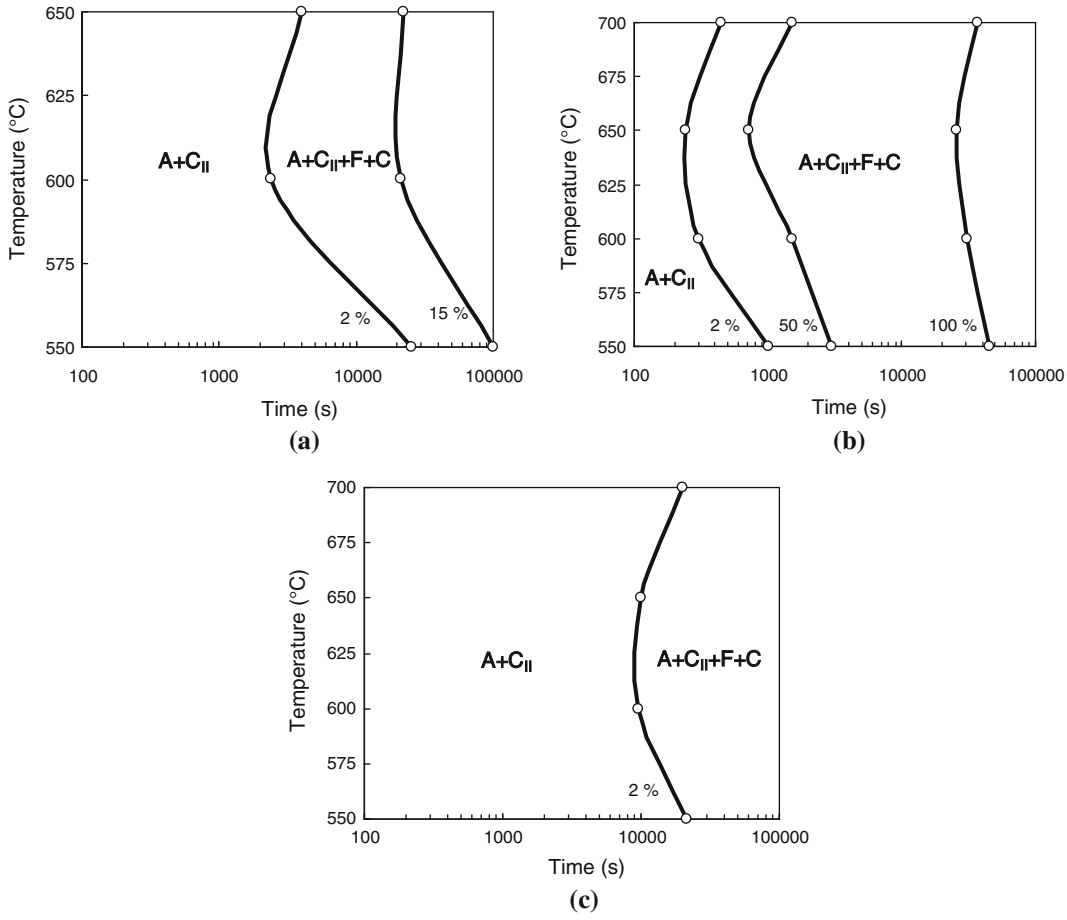

Fig. 10—TTT diagrams for destabilized alloys (*a*) A, (*b*) B, and (*c*) C.

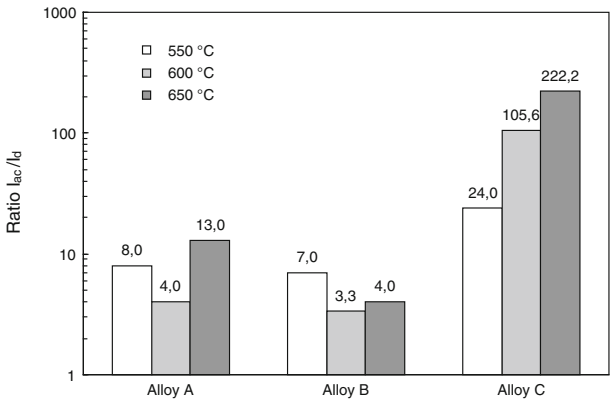

Fig. 11—Ratio $I_{a\text{-}c}/I_d$ for alloys A through C soaked at 823 K to 923 K (550 °C to 650 °C).

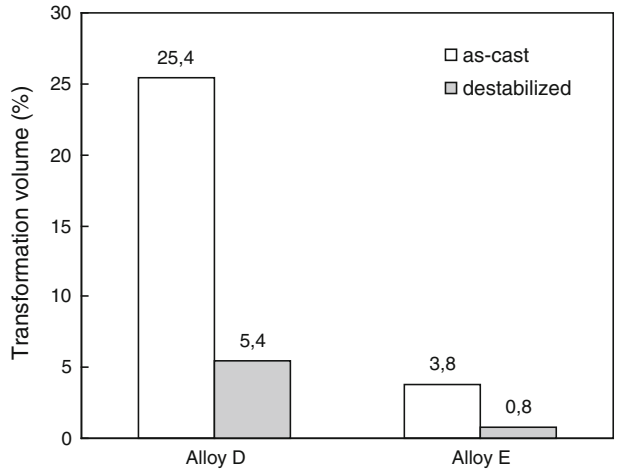

Fig. 12—Pearlite transformation volume in as-cast and destabilized alloys D and E after soaking at 923 K (650 °C), 3 h.

correlation between destabilizing soaking time and secondary carbide precipitation volume in high-Cr cast irons. Based on this finding, it can be supposed that Figure 13 shows the relationships between precipitate volume and subsequent pearlite transformation volume. It also should be highlighted that DIETD is most notable for the first 0.5 to 1.0 hour of soaking, *i.e.*, when a greater part of secondary carbides precipitated in the structure (Figure 3(d)).

F. *Effect of Destabilization on Matrix Chemical Composition Change*

Considering the importance of DIETD for phase transformation in high-Cr cast irons, an attempt to explain this phenomenon was made in the present work. Two main factors that may be responsible for DIETD

were suggested. These are the change of metallic matrix chemical composition and the occurrence of stresses induced by secondary carbide precipitation.

To explore the chemical composition of the metallic matrix, the SEM observation accompanied by EDS analysis was applied. Two specimens of alloy A were used; the as-cast specimen was compared with the specimen soaked for 6 hours at 1223 K (950 °C). Long soaking was applied in order to coarse secondary carbides so as to find sufficiently large places within the matrix for microanalyses detecting. The results of matrix EDS analysis are presented in Table II.

The results from Table II show that the secondary carbides precipitation caused matrix depletion with chromium from 7.31 to 5.00 wt pct due to chromium segregation in secondary carbides. The matrix enrichment by Si, Ni was also detected. Silicon and nickel are known to be graphitizing elements that are rejected from growing carbides into the matrix during precipitation.[7] The ratio "destabilized/as-cast" for Si, Cr, and Ni concentration is 1.26, 0.81, and 1.71, respectively. According to the Mn concentration ratio (1.05), one can say that the change of manganese content in the matrix was negligible.

A decrease of chromium content in austenite is expected to accelerate pearlite transformation, although an increase in the content of other elements has to rise austenite stability to transformation.[25] In order to evaluate the resulting influence of changes in chemical composition on austenite stability, we applied an approach based on the Grossman method for mathematical prediction of an alloy's hardenability.[29] It is known that hardenability is closely associated with the kinetics of austenite-pearlite (bainite) transformation.[25] The Grossman method implies calculation of an ideal critical diameter using a multiplying factor of alloying elements (MF_i) from the formula

$$D_I = D_{IC} \cdot F \qquad [1]$$

where D_{IC} is the ideal critical diameter for carbon content, F is the factor of the influence of the complex alloying elements ($F = (MF_{Mn})\cdot(MF_{Si})\cdot(MF_{Ni})\cdot\ldots$).

Factor F gives the integral influence of all alloying elements dissolved in austenite on its stability to pearlite (bainite) transformation. The values of MF_{Mn}, MF_{Si}, MF_{Ni}, and MF_{Cr} for the average element content (Table II) were found from Figure 5 in Reference 29; the extrapolation for finding F_{Cr} value was applied. The calculations showed that the F value for the destabilized condition is 28 pct higher than the F value for the as-cast condition (260.6 and 203.8 mm, respectively), which allows us to conclude that destabilized austenite should be more resistant to pearlite transformation compared to the as-cast condition. However, the ratio $F_{dest.}/F_{as\text{-}cast}$ (1.28) seems to be insufficient to explain the sharp inhibition of pearlite transformation after destabilization. Therefore, we assumed that there was another factor causing DIETD, namely, the stresses induced by secondary carbides precipitation.

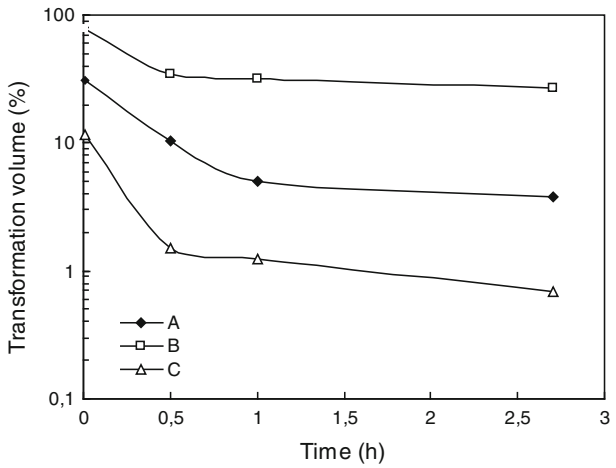

Fig. 13—Effect of destabilization soaking at 1223 K (950 °C) on pearlite transformation volume after subcritical soaking at 923 K (650 °C) for 3 h.

G. *The Evaluation of Stresses Induced by Secondary Carbide Precipitation*

The stresses applied are known to significantly affect phase transformations in alloys.[30–32] Pagounis and Lindroos[32] previously pointed out that second-phase inclusions (Al_2O_3, spinels, TiC, TiN, *etc.*) may cause internal stresses in iron-based alloys during heat treatment. The reason is that particles have a significantly lower TEC than the iron alloy matrix. Based on this approach, we supposed that secondary carbide precipitation in high-Cr cast irons is able to induce stresses, leading to pearlite transformation deceleration. Chromium carbides have higher specific volume compared to austenite: 0.149701 and 0.12528 sm^3/g, respectively. Thus, during precipitation, austenite has to be deformed by secondary carbide particles, leading to the appearance of compressive stresses. However, it is very likely that stresses mostly relax due to high austenite plasticity at the destabilization temperature. When destabilized cast iron is cooled to a subcritical temperature interval,

Table II. Chemical Composition of Metallic Matrix within Dendrite Areas of the Alloy A (Weight Percent)

Specimens Features	Si	Cr	Mn	Ni
As-cast (*a-c*)	0.73 to 0.90	7.02 to 7.64	1.28 to 1.68	0.72 to 1.13
Average value	0.82 ± 0.0531	7.31 ± 0.230	1.47 ± 0.145	0.92 ± 0.173
Destabilized (*d*)	0.92 to 1.14	4.32 to 7.15	1.31 to 2.36	1.06 to 2.08
Average value	0.99 ± 0.049	5.00 ± 0.535	1.56 ± 0.159	1.57 ± 0.095
Ratio *d*/*a-c*	1.26	0.81	1.05	1.71

the stresses show up again because of the differences in the thermal expansion coefficient for austenite (α_A) and secondary carbides (α_C), which are $18.6 \cdot 10^{-6}$ and $10.3 \cdot 10^{-6}$ K^{-1}, respectively.[33] The value of the stress can be calculated approximately as

$$\sigma = \frac{\Delta t \cdot E_A \cdot (\alpha_A - \alpha_C)}{1 - \nu} \quad [2]$$

where Δt is the difference between the destabilization temperature [1223 K (950 °C)] and the pearlite transformation start temperature [~973 K (700 °C)], E_A is the Young's modulus, and ν is the Poisson's ratio.

Assuming that $E_A = 200$ GPa, $\nu = 0.3$, and $\Delta t = 523$ K (250 °C), the stress value calculated according to Eq. [2] is 431.3 MPa. As long as austenite plasticity at 973 K (700 °C) is much lower than that at 1223 K (950 °C), it can be suggested that stresses might not be relieved completely.

Applied stresses may inhibit reconstructive transformation by means of decreasing the carbon atom diffusion and interfacial boundary movement. Because it is destabilized, cast iron C (alloyed by Mn-Mo-Cu) performs the lowest rate of pearlite transformation. One can assume that the higher stability of this cast iron is caused by higher stresses due to additional lattice microdistortions induced by the formation of coherent Cu-enriched precipitates during destabilizing heating.

As the austenite volume is decreased faster during cooling, the appearance of tensile stresses might be expected. Although it is well known that stresses considerably affect phase transformation, there is contradicting information about the influence of the stress mode on transformation kinetics.[34,35] According to Reference 36, the deceleration of pearlite (bainite) transformation takes place just under the compressive stresses applied. In contrast, Weijuan and Shoubin showed that compressive stresses lead to acceleration of bainite reaction in carbon steel.[37] Therefore, more detailed investigations should be fulfilled to determine the mode of stresses induced by secondary carbide precipitation as well as its influence on phase transformation concerning high-chromium cast irons.

The DIETD phenomenon should be considered as an important feature of high-Cr cast irons, because it can significantly affect the casting properties after heat treatment. The point is that destabilization followed by subcritical treatment or slow cooling inside the switched-off furnace is often proposed for softening of high-Cr cast irons to make their machining easy.[18] The sufficient machinability of these alloys can be obtained only if austenite fully transforms onto pearlite, which is accompanied by carbide coagulation. According to Reference 1, the presence of austenite or martensite in the microstructure leads to extremely poor machinability of high-Cr cast irons. Based on the results obtained, one can conclude that the D-S heat treatment or destabilization followed by slow cooling must not be used as a softening treatment because of increasing austenite stability to pearlite transformation. Otherwise, austenite remains in the structure at subcritical temperatures and, on being cooled to ambient temperature, transforms into martensite, which could result in an increase of the casting's bulk hardness, which results in extremely low machinability. Thereby, the probability of manifestation of DIETD must necessarily be taken into account when the heat treatment of high-Cr cast irons is being chosen, especially for cast irons complex alloyed by 3 to 6 wt pct of austenite-stabilizing elements (Mn, Ni, Cu). The alloys mentioned are not recommended to be subjected to high-temperature destabilization during softening heat treatment.

IV. CONCLUSIONS

The effect of destabilizing high-temperature heat treatment on kinetics of pearlite transformation in white high Cr cast irons additionally alloyed by Mn, Mn-Ni-Mo, or Mn-Cu-Mo complex was investigated. The results obtained can be summarized as follows.

1. Destabilizing heat treatment at 1073 K to 1323 K (800 °C to 1050 °C) of as-cast cast irons leads to decomposition of primary austenite affecting the secondary carbide precipitation and increasing the bulk hardness. The precipitation kinetics is presented by TTT diagrams according to which the maximum precipitation rate for all high-chromium cast irons studied is attributed to soaking at 1223 K (950 °C).
2. In all alloys studied, only the "austenite → pearlite" transformation takes place at subcritical isothermal soaking (at 823 K to 973 K (550 °C to 700 °C)). Bainite transformation or secondary carbide precipitations were not found during 25 hours of soaking. TTT diagrams for the γ-Fe → α-Fe phase transformation in subcritical temperatures are built both for as-cast and destabilized states.
3. The destabilization-induced effect of transformation deceleration was found in all of the alloys studied. It is shown that destabilizing heat treatment significantly slows pearlite transformation at 823 K to 973 K (550 °C to 700 °C). The deceleration effect is higher in cast irons alloyed by complex Mn-Ni-Mo or Mn-Cu-Mo. This effect is found to depend on the secondary carbide precipitation volume.
4. The enrichment of austenite by Ni, Si and depletion by Cr takes place in alloy A during destabilizing heat treatment. The summarizing effect of the chemical composition change is estimated to slightly decelerate pearlite transformation kinetics due to certain increase in austenite hardenability. The DIETD phenomenon can be explained also by stresses induced by secondary carbide precipitation because of the difference in the thermal expansion coefficient for austenite and secondary carbides.
5. Destabilization of high-chromium cast irons alloyed by 3 to 6 wt pct of Mn (Mn-Ni-Mo, Mn-C-Mo) during softening heat treatment to improve machinability is not recommended. Destabilization inhibits "austenite → pearlite" transformation; thus, austenite transforms into martensite followed by an

increase of bulk hardness that can have a negative effect on the machinability of cast irons.

ACKNOWLEDGMENTS

Financial support from the Muroran Institute of Technology is gratefully acknowledged. We extend our special thanks to Anatolii Rud and Galina Shendrick, Department of Translation, Pryazovskyi State Technical University, who offered translation support, bettering the English version of this article.

REFERENCES

1. I.I. Tsypin: *Wear-Resistant White Cast Irons. Structure and Properties*, Metallurgical Publishing House, Moscow, 1983, pp. 150–70 (in Russian).
2. R.W. Durman: *Int. J. Miner. Proc.*, 1988, vol. 22, pp. 381–99.
3. E. Zumelzu, I. Goyos, C. Cabezas, O. Optitz, and A. Parada: *J. Mater. Process. Technol.*, 2002, vol. 128 (1–3), pp. 250–55.
4. O.N. Dogan, J.A. Hawk, and G. Laird, II: *Metall. Mater. Trans. A*, 1997, vol. 28A, pp. 1315–28.
5. C.P. Tabrett and I.R. Sare: *Scripta Mater.*, 1998, vol. 38, pp. 1747–53.
6. W. Jun, S. Zhiping, Z. Rulin, L. Cong, S. Baoluo, G. Shenji, and H. Sijiu: *J. Mater. Eng. Perform.*, 2006, vol. 15, pp. 316–19.
7. G. Laird, II: *AFS Trans.*, 1991, vol. 99, pp. 339–57.
8. S. Inthidech, K. Boonmak, P. Sricharoenchai, N. Sasaguri, and Y. Matsubara: *Mater. Trans.*, 2010, vol. 51 (7), pp. 1264–71.
9. A.E. Karantzalis, A. Lekatou, and H. Mavros: *J. Mater. Eng. Perform.*, 2009, vol. 18 (2), pp. 174–81.
10. A. Bedolla-Jacuinde, L. Arias, and B. Hernandez: *J. Mater. Eng. Perform.*, 2003, vol. 12 (4), pp. 371–82.
11. A.E. Karantzalis, A. Lekatou, and E. Diavati: *J. Mater. Eng. Perform.*, 2009, vol. 18 (8), pp. 1078–85.
12. W. Jun, L. Cong, L. Haohuai, Y. Hongshan, S. Baoluo, G. Shenji, and H. Sijiu: *Mater. Charact.*, 2006, vol. 56, pp. 73–78.
13. A.E. Karantzalis, A. Lekatou, A. Kapoglou, H. Mavros, and V. Dracopoulos: *J. Mater. Eng. Perform.*, 2012, vol. 21 (6), pp. 1030–39.
14. D. Kmetic, F. Mlakar, V. Tucič, J. Žvokelj, F. Vodopivec, M. Jakupovič, and B. Ralič: *Železarski Zbornik*, 1987, vol. 21 (4), pp. 151–65.
15. G.L.F. Powell and G. Laird, II: *J. Mater. Sci.*, 1992, vol. 27, pp. 29–35.
16. F. Maratray: *Trans. AFS*, 1971, vol. 79, pp. 121–24.
17. A. Wienngmoon, T. Chairuangsri, and J.T.H. Pearce: *Iron Steel Inst. Jpn. Int.*, 2004, vol. 44 (2), pp. 396–403.
18. P. Amorim, H. Santos, J. Santos, S. Coimbra, and C. Sá: *Mater. Sci. Forum*, 2004, vols. 455–456, pp. 290–94.
19. W.W. Cias: *Trans. AFS*, 1974, vol. 82, pp. 317–28.
20. E.V. Rozhkova, M.E. Garber, and I.I. Tsypin: *Met. Sci. Heat Treatment*, 1981, vol. 23 (1), pp. 59–63.
21. E.V. Rozhkova, S.S. Mikhailovskaya, and I.I. Tsypin: *Met. Sci. Heat Treatment*, 1983, vol. 25 (4), pp. 277–81.
22. G. Laird, II and G.L.F. Powell: *Metall. Trans. A*, 1993, vol. 24A, pp. 981–88.
23. W. Fu, Z. Wang, T. Jing, and Y. Zheng: *J. Mater. Sci Technol.*, 1998, vol. 14, pp. 478–80.
24. O. Erić, D. Rajnović, S. Zec, L. Sidjanin, and M.T. Jovanović: *Mater. Charact.*, 2006, vol. 57 (4–5), pp. 211–17.
25. V.S. Mes'kin: *Basis of Steel Alloying*, Metallurgical Publishing House, Moscow, 1964, pp. 124–179 (in Russian).
26. J. Chen, S. Tang, Z. Liu, and G. Wang: *Mater. Design*, 2013, vol. 49, pp. 465–70.
27. J.D.B. DeMello, M. Durand-Charre, and S. Hamar-Thibault: *Metall. Trans. A*, 1983, vol. 14A, pp. 1793–01.
28. Y. Yokomizo, K. Yamamoto, N. Sasaguri, and Y. Matsubara: *Key Eng. Mater.*, 2010, vol. 457, pp. 237–42.
29. *Steel Castings Handbook*, Suppl. 11, *Hardenability and Heat Treatment*, SFSA, 1985, pp. 3–10.
30. J.G. Wang, L.C. Zhang, G.L. Chen, and H.Q. Ye: *J. Mater. Sci.*, 1998, vol. 33, pp. 2563–71.
31. M. Dalgic and G. Löwisch: *J. Heat Treatment Mater.*, 2004, vol. 1, pp. 28–34.
32. E. Pagounis and V.K. Lindroos: *Scripta Mater.*, 1997, vol. 37 (1), pp. 65–69.
33. *ASM Ready Reference: Thermal Properties of Metals*, ASM INTERNATIONAL, Materials Park, OH, 2002, pp. 12–13.
34. M.C. Uslu, D. Canadinc, H.-G. Lambers, S. Tschumak, and H.J. Maier: *Model. Simul. Mater. Sci. Eng.*, 2011, vol. 19 (4), pp. 045007–23.
35. P.H. Shipway and H.K.D.H. Bhadeshia: *Mater. Sci. Eng., A*, 1995, vol. 201 (1–2), pp. 143–49.
36. E.A. Rumiantzev, V.F. Saveliev, and V.M. Sagalevich: *Met. Sci. Heat Treatment*, 1983, vol. 2, pp. 39–41 (in Russian).
37. L. Weijuan and Z. Shoubin: *Advances in Intelligent and Soft Computing*, Polish Academy of Science, Poland, 2012, vol. 114, pp. 261–68.